# Effects of RFRP-3 on an ovariectomized estrogen-primed rat model and HEC-1A human endometrial carcinoma cells

XUEYING ZHAO[1*], LINA SI[2*], LIN NIU[2], MENG WEI[2], FENGXIA WANG[2], XIAOCHAO LIU[2], ZHIHONG CHEN[2], YUEBING QIAO[2], LUYANG CHENG[1] and SONGHE YANG[2]

Departments of [1]Immunology and [2]Human Anatomy, Chengde Medical University, Chengde, Hebei 067000, P.R. China

Received September 25, 2021; Accepted November 10, 2022

DOI: 10.3892/etm.2022.11775

**Abstract.** The hypothalamic peptide gonadotropin inhibitory hormone (GnIH) is a relatively novel hypothalamic neuropeptide, identified in 2000. It can influence the hypothalamic-pituitary-gonadal axis and reproductive function through various neuroendocrine systems. The present study aimed to explore the effects and potential underlying molecular mechanism of RFamide-related peptide-3 (RFRP-3) injection on the uterine fluid protein profile of ovariectomized estrogen-primed (OEP) rats using proteomics. In addition, the possible effects of RFRP-3 on the viability and apoptosis of the human endometrial cancer cell line HEC-1A and associated molecular mechanism were investigated. The OEP rat model was established through injection with GnIH/RFRP-3 through the lateral ventricle. At 6 h after injection, the protein components of uterine fluid of rats in the experimental and control groups were analyzed using liquid chromatography (LC)-tandem mass spectrometry (MS/MS). Differentially expressed proteins (DEPs) were analyzed using the Gene Ontology (GO) and Kyoto Encyclopedia of Genes and Genomes (KEGG) databases. Protein-protein interactions (PPI) were investigated using the STRING database. PPI networks were then established before hub proteins were selected using OmicsBean software. The expression of one of the hub proteins, Kras, was then detected using western blot analysis. Cell Counting Kit-8, Annexin V-FITC/PI, reverse transcription-quantitative PCR and western blotting were also performed to analyze cell viability and apoptosis. In total, 417 DEPs were obtained using LC-MS/MS, including 279 upregulated and 138 downregulated proteins. GO analysis revealed that the majority of the DEPs were secretory proteins. According to KEGG enrichment analysis, the DEPs found were generally involved in tumor-associated pathways. In particular, five hub proteins, namely G protein subunit α (Gna)13, Gnaq, Gnai3, Kras and MMP9, were obtained following PPI network analysis. Western blot analysis showed that expression of the hub protein Kras was downregulated following treatment with 10,000 ng/ml RFRP-3. RFRP-3 treatment (10,000 ng/ml) also suppressed HEC-1A cell viability, induced apoptosis, downregulated Bcl-2 and upregulated Bax protein expression, compared with those in the control group. In addition, compared with those in the control group, RFRP-3 significantly reduced the mRNA expression levels of PI3K, AKT and mTOR, while upregulating those of LC3-II. Compared with those in the control group, RFRP-3 significantly decreased the protein expression levels of PI3K, AKT, mTOR and p62, in addition to decreasing AKT phosphorylation. By contrast, RFRP-3 significantly increased the LC3-II/I ratio and G protein-coupled receptor 147 (GPR147) protein expression. In conclusion, the present data suggest that RFRP-3 can alter the protein expression profile of the uterine fluid of OEP rats by upregulating MMP9 expression whilst downregulating that of key hub proteins Gna13, GnaQ, Gnai3 and Kras. Furthermore, RFRP-3 can inhibit HEC-1A cell viability while promoting apoptosis. The underlying molecular mechanism may involve activation of GPR147 receptor by the direct binding of RFRP-3, which further downregulates the hub protein Kras to switch on the PI3K/AKT/mTOR pathway. This subsequently reduces the Bcl-2 expression and promotes Bax expression to induce autophagy.

*Correspondence to:* Mrs. Luyang Cheng, Department of Immunology, Chengde Medical University, Anyuan Road, Shuangqiao, Chengde, Hebei 067000, P.R. China
E-mail: chengll526@126.com

Mr. Songhe Yang, Department of Human Anatomy, Chengde Medical University, Anyuan Road, Shuangqiao, Chengde, Hebei 067000, P.R. China
E-mail: 32568666@qq.com

*Contributed equally

*Key words:* gonadotropin inhibitory hormone, uterine fluid, bioinformatics analysis, HEC-1A cells

## Introduction

Success in reproduction is dependent on the ordered regulation of hormone and neuropeptide production in the hypothalamic-pituitary-gonadal (HPG) axis. The main hypothalamic peptide gonadotropin-releasing hormone (GnRH) exerts particularly important functions in driving this axis (1). GnRH is normally produced by the hypophysial portal system to stimulate gonadotropin production (1). In 2009, Tsutsui (2) first demonstrated that a previously unknown

hypothalamic neuropeptide was able to inhibit gonadotropin production in Japanese quail, which was referred to as gonadotropin-inhibitory hormone (GnIH). Subsequently, existence of GnIH orthologs, such as RFamide-related peptide (RFRP)-1 and -3, were revealed in numerous vertebrates. RFRP-3 serves a particularly key role and has been extensively studied (3). GnIH exerts an important role in the suppression of reproduction, specifically by acting on GnRH neurons and pituitary glands (4,5), through G protein-coupled receptor 147 (GPR147) (4,5). GnIH/RFRP-3 has been previously suggested to inhibit the immediate peripheral effects on vertebrate gonads (6). The expression of GnIH and its receptor can be detected within germ and steroidogenic cells in bird or mammal gonads, where it potentially suppresses gonadal steroid production to prevent the maturation and differentiation of germ cells in either an autocrine or paracrine manner (6). The uterus is an important reproductive organ in female mammals. Han *et al* (7) previously suggested that the intracerebroventricular (ICV) injection of RFRP-3 can delay uterine development. Therefore, it would be of interest to examine the molecular mechanism by which GnIH can regulate uterus function.

According to previous studies, GnIH can directly regulate the function of pro-opiomelanocortin (POMC), neuropeptide Y (NPY) and kisspeptin neurons of opioid melanocytes, by inhibiting the expression of POMC and kisspeptin whilst increasing that of NPY (8-10). In addition, POMC, NPY and kisspeptin neurons have been shown to directly mediate effects on the GnRH neurons and modulate the reproductive function by regulating GnRH synthesis (11-13). Therefore, GnIH appear to confer both direct and indirect effects on hypothalamic GnRH neurons, mainly by reducing pituitary gonadotropin release through inhibiting POMC and kisspeptin neurons whilst promoting NPY neurons. This ultimately affects the HPG axis and downstream target organs, such as the uterus. However, it remains unclear if GnIH can regulate the uterus through the HPG reproductive axis.

Endometrial cancer (EC) is one of the most common malignancies of the female reproductive system that can be lethal (14). In recent years, alongside the increasing incidence of obesity, the worldwide incidence of EC has also been increasing on an annual basis, particularly among younger women (15). Treatment of EC is difficult due to the simultaneous need for preserving patient fertility (16). Therefore, hormone adjuvant therapy has been garnering attention due to its advantages of low toxicity, reduced severity of side effects, maneuverability and favorable safety profiles (14,15). A previous study has found that GnRH analogues can stimulate the HPG axis to reduce the secretion of luteinizing hormone (LH) and follicle-stimulating hormone (FSH), which suppresses gonadal function and indirectly inhibits tumor growth (17). In addition, GnRH agonists can reduce the proliferation of human EC cells in a dose- and time-dependent manner (18,19). By contrast, GnRH antagonists can induce apoptosis in human EC cells by activating p38 MAPK and JNK signaling, in addition to the proapoptotic protein Bax (20). This strategy of reversible medical has been successfully introduced into the treatment regimen of EC, where the underlying mechanism is consistent with the biological characteristics of GnIH (17-20). Therefore, GnIH may provide a novel avenue for developing a treatment strategy for EC.

In the present study, the potential effects of GnIH/RFRP-3 injection through the lateral ventricle on the uterus of ovariectomized estrogen-primed (OEP) rats were investigated using liquid chromatography (LC)-tandem mass spectrometry (MS/MS) analysis. Using these data, the differentially expressed proteins (DEPs) were selected, which were subjected to Gene Ontology (GO) functional annotation and Kyoto Encyclopedia of Genes and Genomes (KEGG) enrichment analyses. Subsequently, their molecular mechanism and clinical values were investigated through protein-protein interaction (PPI) network analysis. Cell Counting Kit-8 (CCK-8) assay, Annexin V-FITC/PI double staining and western blot analysis were used to assess the effects of RFRP-3 on the apoptosis of HEC-1A cells. Findings from the present study may provide novel ideas for examining the effects of GnIH on reproduction.

## Materials and methods

*Study animals and model establishment*. In total, 30 female Sprague-Dawley rats (age, 6-7 weeks; weight, 180-220 g) were provided by Beijing Huafukang Biotechnology Co., Ltd. (animal certification no. 11401300067446). These animals were fed with normal diet and maintained at 22-25˚C, in a natural light/dark cycle (12/12 h), the relative humidity of the animal facility was 40-70%, with free access to food and water for 1 week before animal experimentation commenced. Animal experimental procedures were performed in accordance with the ethical standards of and approved by The Experimental Animal Welfare Ethics Committee of Chengde Medical University (Chengde, China).

The rat ovariectomized estrogen-primed (OEP) model was established. Briefly, the rats were anesthetized with 10% chloral hydrate (300 mg/kg) before being bilaterally ovariectomized or in all anesthetic procedures under sterile conditions. None of the rats exhibited any signs of peritonitis, pain or discomfort during the operation. After 15 days, the animals were subjected to a subcutaneous injection of estradiol benzoate [Shanghai full woo Biotechnology (Zhumadian) Co., Ltd.; 1 mg/kg/day] for 5 days. This drug was given to keep the estrogen level in each rat consistent and eliminate the influence of estrogen on GnIH. Animal status was monitored daily. The animals were then randomly divided into the following two groups: i) RFRP-3 group (n=15), in which RFRP-3 (16 $\mu$l/kg; final concentration, 2 $\mu$g/$\mu$l; solvent, normal saline; Bachem AG) was injected into the lateral ventricle of the rats following anesthesia as aforementioned; and ii) normal saline injection group (n=15), in which saline was injected into the lateral ventricle of rats. The uterine fluid of five rats from the experiment and control groups was mixed and divided into three parts, which were stored in liquid nitrogen. Euthanasia was performed by cervical dislocation, before which the animals were anesthetized, and 6 h after administration, uterine fluid samples were collected. The chest was opened to verify death of each animal, where absence of any fluctuations in the chest caused by breathing and heartbeat was verified.

The humane endpoints used to determine when the animal must be immediately euthanized were as follows: i) Rapid weight loss of 15-20%; ii) lack of food and drinking water intake; iii) in the state of non-anesthesia or sedation, when

animal mental depression is accompanied by hypothermia; and iv) abnormal central nervous responses (convulsions, tremors, paralysis, head tilt).

*Cell lines*. Human EC HEC-1A cells were provided by Procell Life Science & Technology Co., Ltd. HEC-1A cells were cultured in McCoy 5A medium [Zhongke Maichen (Beijing) Technology Co., Ltd.], supplemented with 15% FBS (Sartorius AG) and 1% penicillin/streptomycin, at 37˚C with 5% $CO_2$.

*Determination of optimal concentration of RFRP-3*. RFRP-3 (Tocris Bioscience) was diluted with PBS to obtain a final concentration of 2 mg/ml as the stock solution and stored at -20˚C. HEC-1A cells were seeded into 96-well plates in triplicates. The cells were then treated with 0 (control), 0.1, 1, 10, 100, 1,000 and 10,000 ng/ml RFRP-3. Cells in the control group were subjected to no treatments, whilst the cells in the treatment groups were incubated with RFRP-3 at the indicated concentrations for 24 h.

*Identification of DEPs*. Peptides were separated via high-performance LC (Agilent 1260 Infinity II LC; Agilent Technologies, Inc.) from uterine fluid. Samples were separated on a XTerra RP18 column (4.6x50 mm; 5 $\mu$m; Waters Corporation) at 35˚C. Mobile phases A and B were comprised of 1,000:1 (v/v) methanol/formic acid and 1,000:1 (v/v) water/formic acid, respectively. The flow rate was 0.4 ml/min. The injection volume was 3 $\mu$l and the total running time was 2 min.

Peptides were identified via MS/MS. Multiple reaction monitoring was performed with an Agilent 6460 triple quadrupole MS/MS fitted with the Agilent Jet Stream Electrospray Ionization probe (Agilent Technologies, Inc.) in the positive ion mode. Data were analyzed using the full scan mass spectra (300-1800 M/z). The mass spectrometry ion source was a nano-ESI ion source, so without parameters such as nitrogen gas temperature, nebuliser pressure and flow rate. Experiments were performed in triplicates. Finally, the mass spectrometry data were analyzed using the Proteome Discoverer software (version 1.4.0.288; Thermo Fisher Scientific, Inc.). DEPs were screened using P<0.05 and Fold Change (FC)=2 as criteria. Protein name, gene ID, molecular weight and other information were obtained using the UniProt knowledgebase (http://www.uniprot.org/).

*Bioinformatics analysis*. GO analysis was performed, including the biological process (BP), cell component (CC) and molecular function (MF), using the GO (http://www.geneontology.org/) online tool. KEGG pathways associated with the DEPs were analyzed using the KEGG (http://www.KEGG.jp) online tool. The dashed blue line indicates P<0.05, the dashed red line indicates P<0.01. The top 10 items were selected according to P<0.01 based on their corresponding enrichment results.

*PPI network of DEPs*. The interaction network of DEPs was searched against the Search Tool for the Retrieval of Interacting Genes/Proteins (STRING; http://string-db.org) database. The STRING database was also utilized to construct the PPI networks of DEPs. Statistical significance was deemed as interaction with a pooled score of >0.4. The PPI network was drawn using the multi-omics data analysis tool, OmicsBean V1.0 (http://www.omicsbean.cn/). The interaction between proteins is shown as a solid line, and proteins and KEGG terms are linked by a dotted line. The protein that interacts most closely with other proteins in the PPI network was selected as the hub protein. It can be seen from the PPI network that the DEPs Gna 13, Gnaq and Gnai3 participate in the platelet activation pathway. In addition, KEGG pathway analysis (https://www.kegg.jp/kegg/) was performed ('platelet activation' was searched for in the PATHWAY database).

*University of Alabama cancer (UALCAN) database analysis*. The UALCAN database (http://ualcan.path.uab.edu/index.html); public datasets name, TCGA Gene (http://ualcan.path.uab.edu/analysis.html); TCGA dataset, uterine corpus endometrial carcinoma public datasets) was used to explore the internal relationship between endometrial cancer and hub proteins (Gna13, Gnaq, Gnai3, Kras and MMP9) that were screened using the PPI network. Gna13, Gnaq, Gnai3, Kras and MMP9 expression was compared between human endometrial carcinoma tissues and normal tissues using The Cancer Genome Atlas (TCGA) database. In the results, only the hub proteins with statistical differences were displayed. The number of normal tissues was 35 and the number of EC tissues was 546.

*CCK-8 assay*. HEC-1A cells were seeded into the 96-well plate at a density of $1x10^4$/well. After 24 h, 100 $\mu$l RFRP-3 at the indicated concentrations (0, 0.1, 1, 10, 100, 1,000 and 10,000 ng/ml) was used to treat the cells for 24 h. After removing the medium, a solution containing 10% CCK-8 (APeXBIO Technology LLC) in McCoy 5A medium was added into each well. The reaction was conducted at 37˚C for 1 h, before the optical density value at 450 nm was measured and recorded. The calculation formula of the viability rate was: [(RFRP-3 group-blank)/(Control-blank)-1] x100%.

*Detection of apoptosis*. Apoptosis of HEC-1A cells was detected by flow cytometry using an Annexin V-FITC/PI apoptosis kit (BD Biosciences). HEC-1A cells were seeded into 6-well plates at a density of $3x10^5$/well and treated with either complete McCoy 5A medium or complete McCoy 5A medium with 10,000 ng/ml RFRP-3 for 24 h. The cells were then suspended in binding buffer and stained with 5 $\mu$l Annexin V-FITC reagent and 5 $\mu$l PI solution at room temperature in dark for 15 min. The stained cells were then analyzed by Coulter ELITEesp flow cytometry (Beckman Coulter, Inc.) and data analysis was performed using FloMax 2.7 software (Sysmex Partec GmbH). In the present study, the sum of late and early apoptotic cells was used as the readout for the apoptotic rate.

*Reverse transcription-quantitative PCR (RT-qPCR)*. Total RNA was extracted from treated HEC-1A cells (control and 10,000 ng/ml RFRP-3 groups) using the Takara MiniBEST Universal RNA Extraction kit (Takara Biotechnology Co., Ltd.), according to the manufacturer's protocol. Concentration of total RNA was determined using NanoDrop™ 2000 (Thermo Fisher Scientific, Inc.), before the RT reaction was

Table I. Top 10 upregulated differentially expressed proteins.

| UniProt ID | Gene name | Protein name (short name, full name) | Log2 fold change | Organism |
|---|---|---|---|---|
| P0CC09 | Hist2h2aa3 | H2A2A_RAT, histone H2A type 2-A | 13.78 | Rattus norvegicus (Rat) |
| P84245 | H3f3b | H33_RAT, histone H3.3 | 13.31 | Rattus norvegicus (Rat) |
| P36953 | Afm | AFAM_RAT, afamin | 12.73 | Rattus norvegicus (Rat) |
| Q62714 | Np4 | DEF4_RAT, neutrophil antibiotic peptide NP-4 | 12.35 | Rattus norvegicus (Rat) |
| P15684 | Anpep | AMPN_RAT, aminopeptidase N | 12.16 | Rattus norvegicus (Rat) |
| Q9QYK2 | Ppargc1a | PRGC1_RAT, peroxisome proliferator-activated receptor gamma coactivator 1-alpha | 12.13 | Rattus norvegicus (Rat) |
| P30349 | Lta4h | LKHA4_RAT, leukotriene A-4 hydrolase | 12.02 | Rattus norvegicus (Rat) |
| Q9R063 | Prdx5 | PRDX5_RAT, peroxiredoxin-5, mitochondrial | 11.81 | Rattus norvegicus (Rat) |
| Q5XHY1 | Carmil3 | LR16B_RAT, leucine-rich repeat-containing protein 16B | 11.79 | Rattus norvegicus (Rat) |
| P20762 | P20762 | IGG2C_RAT, Ig gamma-2C chain C region | 11.72 | Rattus norvegicus (Rat) |

performed using the Prime Script™ RT reagent Kit (Takara Bio, Inc.) according to the manufacturer's instructions. qPCR was performed using the TB Green™ Premix ExTaq™ II kit (Takara Bio, Inc.) on a CFX96 Real-Time PCR Detection System (Bio-Rad Laboratories, Inc.). The thermocycling conditions were as follows: Initial denaturation step at 95˚C for 30 sec, followed by 40 cycles of denaturation at 95˚C for 5 sec, and annealing and extension at 60˚C for 30 sec. The primer sequences were as follows: PI3K forward, 5'-GGAATG CTGCAAGATCAAGAAA-3' and reverse, 5'-TTGGTGGTA ATGGAAGAGGAAGA-3'; AKT forward, 5'-CTTGCTTTC AGGGCTGCTCA-3' and reverse, 5'-TACACGTGCTGCCAC ACGATAC-3'; mTOR forward, 5'-CTTGCTGAACTGGAG GCTGATGG-3' and reverse, 5'-CCGTTTTCTTATGGGCTG GCTCTC-3'; LC3-II forward, 5'-gtCagCgTctCcACACCA ATCTC-3' and reverse, 5'-TCCTGGGAGGCATAGaCCATG TAC-3'; and GAPDH forward, 5'-GCACCGTCAAGGCTG AGAAC-3' and reverse, 5'-TGGTGAAGACGCCAGTGGA-3'. The relative expression levels of target genes were calculated using the $2^{-\Delta\Delta Cq}$ (Livak) method (21). GAPDH was used as internal reference.

*Western blot analysis*. HEC-1A cells (control and RFRP-3 groups) were lysed using RIPA lysis buffer (Beijing Solarbio Science & Technology Co., Ltd.). Protein concentrations were measured using a BCA kit. A total of 30 $\mu$g protein per lane was separated by 10-12% SDS-PAGE and then transferred onto PVDF membranes. The membranes were then blocked with 5% skimmed milk at room temperature for 2 h, before being incubated with primary antibodies against GAPDH (rabbit; 1:6,000; cat. no. ab9485; Abcam), Kras (rabbit; 1:2,000; cat. no. ab191595; Abcam), Bcl-2 (rabbit; 1:800; cat. no. ab59348; Abcam), Bax (rabbit; 1:800; cat. no. ab32503; Abcam), PI3K (rabbit; 1:500; cat. no. AP0231; Bioworld Technology, Inc.), AKT (rabbit; 1:10,000; cat. no. ab179463; Abcam), phosphorylated (p)-AKT (rabbit; 1:2,000; cat. no. 4060; Cell Signaling Technology, Inc.), mTOR (rabbit; 1:2,000; cat. no. ab32028; Abcam), LC3B (rabbit; 1:2,000; cat. no. ab192890; Abcam), p62 (rabbit; 1:1,000; cat. no. A19700; ABclonal Biotech Co., Ltd.) and GPR147 (also referred to as NPFF-1 receptor; rabbit; 1:5,00; cat. no. bs-12018R; Beijing Bioss Biotechnology Co., Ltd.) at 4˚C overnight. After TBST washing, the membranes were incubated with the corresponding HRP-conjugated secondary antibodies (rabbit; 1:8,000; cat. no. ab205718; Abcam) for another 1 h at room temperature. Immune-reactive proteins were visualized with the ECL luminescence reagent (cat. no. MA0186; Dalian Meilun Biology Technology Co., Ltd.). Protein band intensities were analyzed and normalized to GAPDH that was used as loading control. A Tanon 5200 imaging system (Tanon Science and Technology Co., Ltd.) was used to detect the bands, and ImageJ 1.52a software (National Institutes of Health) was used to semi-quantify the integrated density.

*Statistical analysis*. Data are expressed as the mean ± standard deviation. Each experiment was carried out three times. Statistical analysis was performed using the SPSS 22 software (IBM Corp.). Comparisons among multiple groups were conducted using one-way ANOVA followed by Dunnett's post hoc test. An unpaired t-test was used to compare the differences between two groups for the results of RT-qPCR and western blotting. $P<0.05$ was considered to indicate a statistically significant difference.

## Results

*Protein profile of uterine fluid is changed by RFRP-3*. Using $P<0.05$ and FC=2 as thresholds, a total of 417 DEPs were identified in the uterine fluid of OEP rats treated with RFRP-3 compared with control rats, including 279 upregulated and 138 downregulated proteins (Tables I and II).

*Analysis of the biological function of DEPs after the ICV injection of RFRP-3*. To analyze the BP, CC and MF terms of DEPs, GO functional annotation was performed (Fig. 1). In terms of BP, DEPs were found to be mostly enriched in 'response to organic substance' (GO ID: GO0010033), 'response to oxygen-containing compound' (GO ID: GO1901700), 'regulation of biological quality' (GO ID: GO0065008) and 'response to external stimulus' (GO ID: 0009605) (Fig. 1A). For MF, the

Table II. Top 10 downregulated differentially expressed proteins.

| UniProt ID | Gene name | Protein name (short name, full name) | Log2 fold change | Organism |
|---|---|---|---|---|
| P04218 | Cd200 | OX2G_RAT, OX-2 membrane glycoprotein | -18.03 | Rattus norvegicus (Rat) |
| Q8K3K9 | Gimap4 | GIMA4_RAT, GTPase IMAP family member 4 | -12.8 | Rattus norvegicus (Rat) |
| B4F795 | Slc44a2 | CTL2_RAT, choline transporter-like protein 2 | -10.95 | Rattus norvegicus (Rat) |
| P14925 | Pam | AMD_RAT, peptidyl-glycine alpha-amidating monooxygenase | -10.65 | Rattus norvegicus (Rat) |
| A9UMV8 | H2afj | H2AJ_RAT, histone H2A.J | -10.47 | Rattus norvegicus (Rat) |
| P33568 | Rb1 | RB_RAT, retinoblastoma-associated protein | -10.05 | Rattus norvegicus (Rat) |
| Q9ESV6 | Gapdhs | G3PT_RAT, glyceraldehyde-3-phosphate dehydrogenase, testis-specific | -9.75 | Rattus norvegicus (Rat) |
| Q08849 | Stx3 | STX3_RAT, syntaxin-3 | -9.41 | Rattus norvegicus (Rat) |
| Q3B8N7 | Tsc22d4 | T22D4_RAT, TSC22 domain family protein 4 | -9.41 | Rattus norvegicus (Rat) |
| Q3KRC4 | Gprc5c | GPC5C_RAT, G-protein coupled receptor family C group 5 member C | -9.2 | Rattus norvegicus (Rat) |

DEPs were particularly enriched in 'protein binding' (GO ID: GO0005515), 'protein complex binding' (GO ID: GO0032403) and 'macromolecular complex binding' (GO ID: GO0044877) (Fig. 1C). In terms of CC, the DEPs were found to be associated with 'extracellular region' (GO ID: GO0005576) and 'membrane-bounded vesicle' (GO ID: GO0031988) (Fig. 1B). The aforementioned results imply that these DEPs participate in protein, polypeptide and carbohydrate metabolism. Furthermore, these proteins exhibited an association with antioxidation and were indicated to regulate cell proliferation, apoptosis, cell migration, cell adhesion and angiogenesis.

*Analysis of signal pathways associated with the DEPs after the ICV injection of RFRP-3*. To further assess the possible functions of DEPs caused by RFRP-3 treatment, signaling pathway enrichment analysis was performed using KEGG pathway analysis (Fig. 2). These DEPs were observed to be enriched in 'carbon metabolism' (pathway ID: rno01200), 'gap junction' (pathway ID: rno04540), 'long-term depression' (pathway ID: rno04730), 'regulation of actin cytoskeleton' (pathway ID: rno04810), 'biosynthesis of amino acids' (pathway ID: rno01230), 'complement and coagulation cascades' (pathway ID: rno04610), 'glycolysis/gluconeogenesis' (pathway ID: rno00010), 'proteoglycans in cancer' (pathway ID: rno05205), 'platelet activation' (pathway ID: rno04611) and 'thyroid hormone synthesis' (pathway ID: rno04918).

*PPI network of the DEPs after the ICV injection of RFRP-3*. PPI analysis was then performed using the STRING database, which was used to build the PPI network (Fig. 3A). OmicsBean was utilized for the visualization of this network (Fig. 3A). In total, five proteins were identified to be hub proteins, namely G protein subunit α (Gna)13, Gnaq, Gnai3, Kras and MMP9. Among them, the protein expression levels of Gna 13, Gnaq, Gnai3 and Kras were decreased, while the protein expression levels of MMP9 were increased. In addition, based on KEGG pathway database analysis, it can be seen that the platelet activation pathway activated the AC/cAMP/PKA signaling pathway (Fig. 3B).

*Expression of Gna13, Gnaq, Kras and MMP9 is significantly changed in EC*. Using the UALCAN database platform, The Cancer Genome Atlas database was screened. The expression of the hub proteins Gna13, Gnaq, Kras and MMP9 was found to be significantly different between EC and the normal tissues (Fig. 4). Specifically, compared with that in normal samples, Kras and MMP9 expression was increased, whereas Gnaq and Gna13 expression was decreased in EC tissues.

*RFRP-3 reduces the expression of Kras in HEC-1A cells*. The expression levels of Kras were examined. As shown in Fig. 5, compared with those in the control group, the expression levels of Kras were significantly reduced in the RFRP-3 group.

*RFRP-3 inhibits the viability of HEC-1A cells*. The potential effects of RFRP-3 on the viability of HEC-1A cells were next investigated using the CCK-8 assay. As shown in Fig. 6 and Table III, compared with that in the control group, cell viability was significantly decreased in the 10,000 ng/ml RFRP-3 treatment group ($P<0.05$). However, the differences in cell viability were not significant between the control group and the 0.1, 1, 10, 100 and 1,000 ng/ml RFRP-3 groups. These results suggest that RFRP-3 at 10,000 ng/ml was able to suppress EC cell viability. Therefore, in subsequent experiments HEC-1A cells were treated with 10,000 ng/ml RFRP-3.

*RFRP-3 induces apoptosis in HEC-1A cells*. To investigate the effects of RFRP-3 on HEC-1A cell apoptosis, flow cytometry was performed. As shown in Fig. 7, the upper right quadrant represents late apoptotic cells, whilst the lower right quadrant represents early apoptotic cells. The proportion of apoptotic cells (%) in the RFRP-3 group was found to be higher compared with that in the control group (Fig. 7A-C). Results from the western blot analysis revealed that compared with those in the control group, Bcl-2 protein expression was significantly lower whereas Bax protein expression was significantly higher in the RFRP-3 group (Fig. 7D and E). These results suggest that RFRP-3 can induce apoptosis in HEC-1A cells.

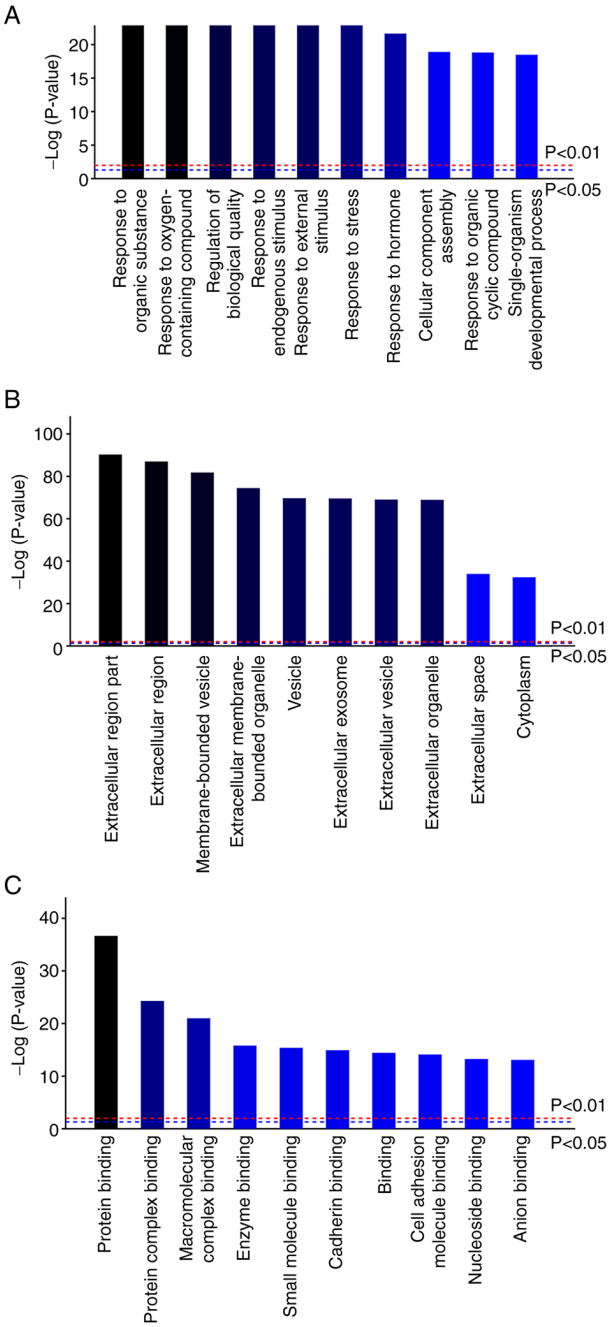


Figure 1. Gene ontology annotations for the differentially expressed proteins. (A) Biological processes. (B) Cell components. (C) Molecular functions. The top 10 items were selected according to P<0.01 based on their corresponding enrichment results. The dashed blue line indicates P<0.05, the dashed red line indicates P<0.01.

*RFRP-3 inhibits the PI3K/AKT/mTOR pathway in HEC-1A cells*. To investigate the effects of RFRP-3 on the PI3K/AKT/mTOR pathway in HEC-1A cells, the expression levels of the associated components were detected using RT-qPCR and western blot analysis. As shown in Fig. 8A, compared with those in the control group, the expression levels of PI3K/AKT/mTOR genes were significantly lower in the RFRP-3 group. Treatment with 10,000 ng/ml RFRP-3 significantly reduced the protein expression levels of PI3K and mTOR whilst also reducing the phosphorylation of AKT, compared with those in the control group (Fig. 8B and C). The expression levels of AKT were similar between the control and RFRP-3 groups. These results suggest that RFRP-3 can inhibit the PI3K/AKT/mTOR pathway to potentially promote tumor apoptosis.

Table III. Effects of RFamide-related peptide 3 on cell viability of HEC-1A cells.

| Group | Viability rate of cells, % | P-value |
|---|---|---|
| Control | 0.000 | |
| 0.1 ng/ml RFRP-3 | 1.560±1.598 | - |
| 1 ng/ml RFRP-3 | 0.960±1.254 | - |
| 10 ng/ml RFRP-3 | -2.250±0.782 | - |
| 100 ng/ml RFRP-3 | -1.983±1.356 | - |
| 1,000 ng/ml RFRP-3 | -3.297±4.085 | - |
| 10,000 ng/ml RFRP-3 | -8.127±2.837 | P<0.05[a] |

[a]Compared with the control group. -, no statistical difference compared with the control group.

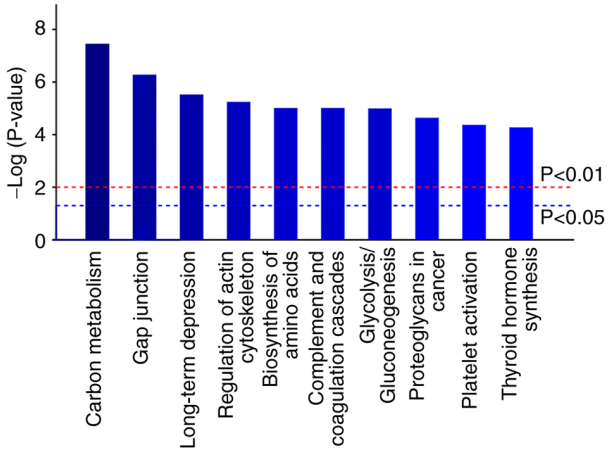


Figure 2. Distribution of the enriched Kyoto Encyclopedia of Genes and Genomes pathways. Columns represent the associated pathways, marked with different colors varying from light blue (low P-values) to dark blue (high P-values). The dashed blue line indicates P<0.05, the dashed red line indicates P<0.01.

*RFRP-3 induces autophagy in HEC-1A cells*. mTOR serves a key role in regulating autophagy. Therefore, the expression levels of associated genes were detected using RT-qPCR and western blot analysis. As shown in Fig. 9A, compared with those in the control group, the mRNA expression levels of LC3-II were significantly higher in the RFRP-3 group. Treatment with 10,000 ng/ml RFRP-3 significantly increased the LC3-II/I protein expression ratio compared with those in the control group. In addition, RFRP-3 treatment significantly reduced p62 expression compared with that in the control group (Fig. 9B and C). The concurrent accumulation of LC3-II and degradation of p62 induced by RFRP-3 suggests that it increased autophagic activity.

*RFRP-3 increases GPR147 protein expression in HEC-1A cells*. To explore the underlying molecular mechanism of

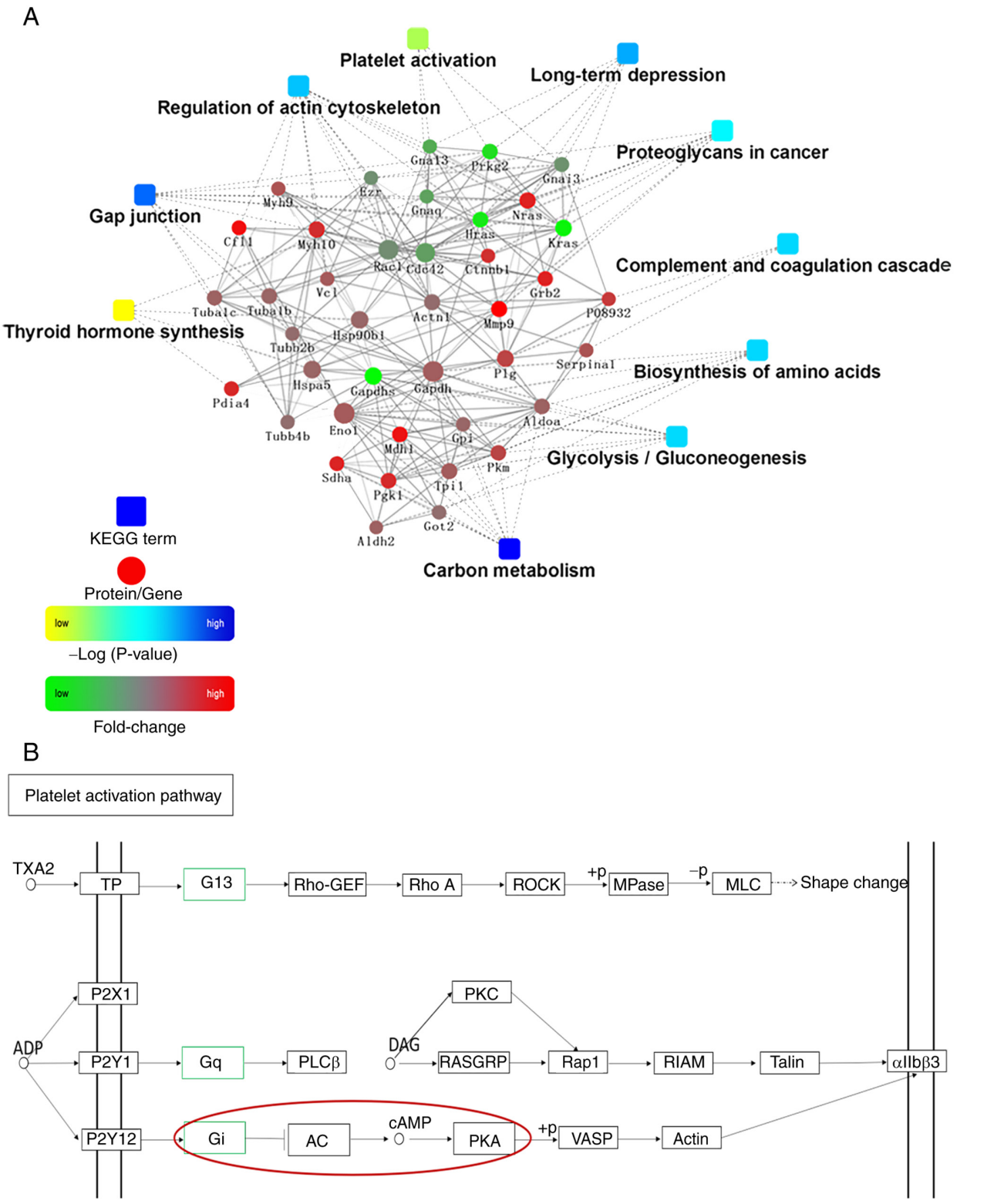


Figure 3. (A) Protein-Protein Interaction network diagram. Circles represents proteins and lines represents interactions between these proteins encoded by the indicated genes. Rectangles indicate the KEGG pathways, marked with different colors ranging from yellow (low P-values) to blue (high P-values). The red nodes represent upregulated proteins, whereas the green nodes represent downregulated proteins. KEGG, Kyoto Encyclopedia of Genes and Genomes. (B) 'Platelet activation pathway'. The green rectangle represents downregulated differential proteins and the red ellipse represents the activated pathway.

RFRP-3, the protein expression of GPR147, one of the potential receptors for RFRP-3, was examined using western blot analysis. As shown in Fig. 10, compared with that in the control group, the expression levels of GPR147 were significantly increased in the RFRP-3 group.

## Discussion

GnIH is a relatively novel hypothalamic neuropeptide, discovered in 2000 (2). GnIH has been previously shown to show a high degree of conservation in vertebrates, from

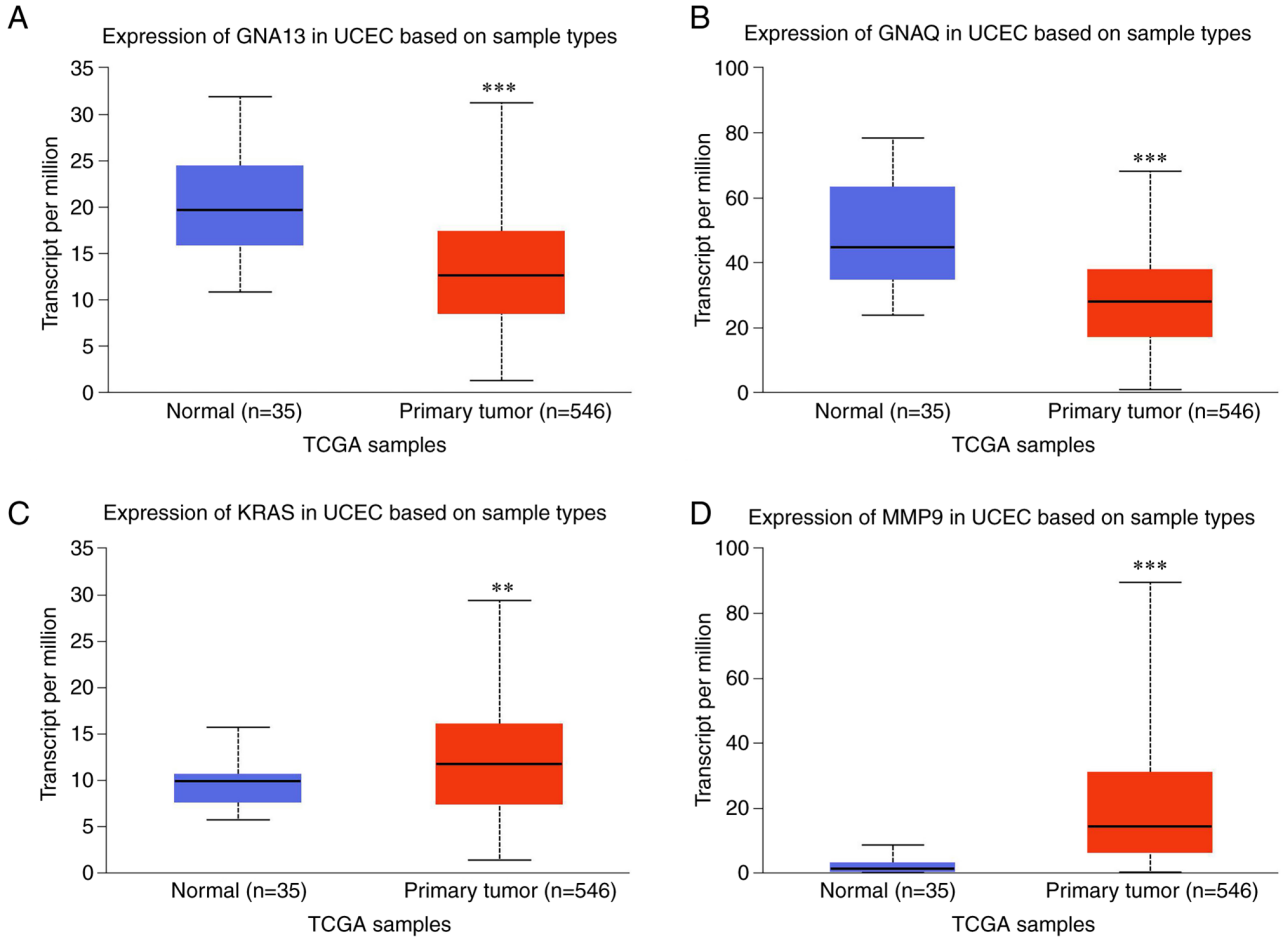


Figure 4. Analysis results of UALCAN database. Expression of (A) Gna13, (B) Gnaq, (C) Kras and (D) MMP9 in UCEC compared with normal tissues. $^{**}$P<0.01 and $^{***}$P<0.001 vs. normal. Gna, G protein subunit α; TCGA, The Cancer Genome Atlas; UCEC, uterine corpus endometrial carcinoma.

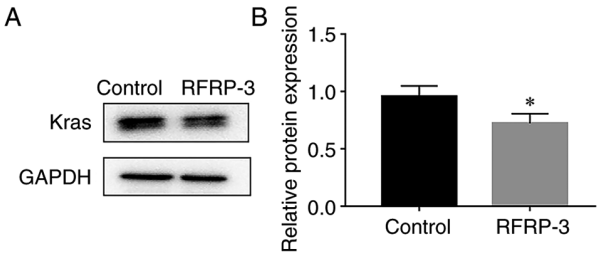


Figure 5. Effects of RFRP-3 on the expression of Kras in HEC-1A cells. The cells in the RFRP-3 group were treated with 10,000 ng/ml RFRP-3 for 24 h. (A) Western blot analysis of Kras expression. Since the Kras antibody used was a recombinant antibody, it may produce non-specific bands (lower band) (67). (B) Semi-quantification of Kras expression, presented as relative expression. $^{*}$P<0.05 vs. control (mean ± SD of control, 0.9553±0.05349; mean ± SD of RFRP-3, 0.7221±0.04802.). RFRP-3, RFamide-related peptide 3.

agnatha to humans (2). In addition, orthologs of GnIH have also been discovered in mammals, referred to as RFRP-1 and RFRP-3 (2). In particular, RFRP-3 has been found to mediate important roles in various biological processes, especially in energy balance, feeding and reproduction (22-27). For GnIH neurons, the cell bodies are localized to the dorsomedial hypothalamic (DMH) area and paraventricular nucleus in the majority of mammals (28). RFRP-3 mRNA expression has previously been detected in the hypothalamus, eyes, ovaries and uterus of juvenile sheep (29). In addition, GnIH is highly expressed in the hypothalamus, pituitary, ovaries, testis and epididymis (30). Li *et al* (31) reported that in sows, GnIH mRNA can be detected in the central nervous system, specifically in the hypothalamus and medulla oblongata. Furthermore, it can be found in the peripheral tissues, such as the ovaries and uterus (31). RFRP mRNA transcripts have also been detected in the hypothalamus of rats and humans (32). GnIH neuronal cell bodies have been observed in the DMH area of the human hypothalamus, where their neural fibers can project into the median eminence external zone (27).

RFRPs are mainly localized in the normal human ovaries, corpus luteum and the large pre-ovulatory follicle granulosa cell layer (27,33). The GnIH receptor mainly mediates the function of GnIH. Bonini *et al* (34) previously detected two G-coupled protein receptors of neuropeptide FF (NPFF). There are C-terminal PQRFamide motifs in NPFF1 (the same as GPR147), NPFF2 (the same as GPR74). GPR147 is considered to be the major GnIH receptor (34). GnIH can exert direct effects on hypothalamic GnRH and pituitary neurons through the GnIH receptor to inhibit the production of gonadotropin and the reproductive function (33,35). It has been shown that the mRNA expression levels of GnIH receptors in rabbits are high, whereas GPR147 mRNA is mainly

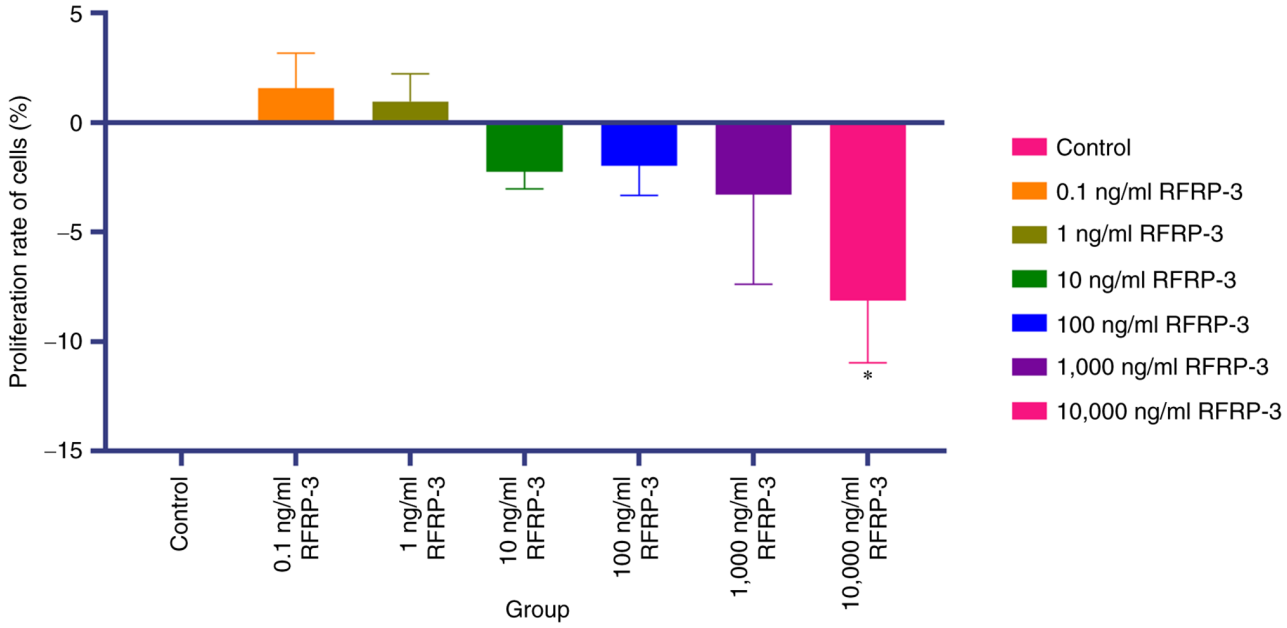


Figure 6. Effects of RFRP-3 on the viability of HEC-1A cells. *P<0.05 vs. control. RFRP-3, RFamide-related peptide 3.

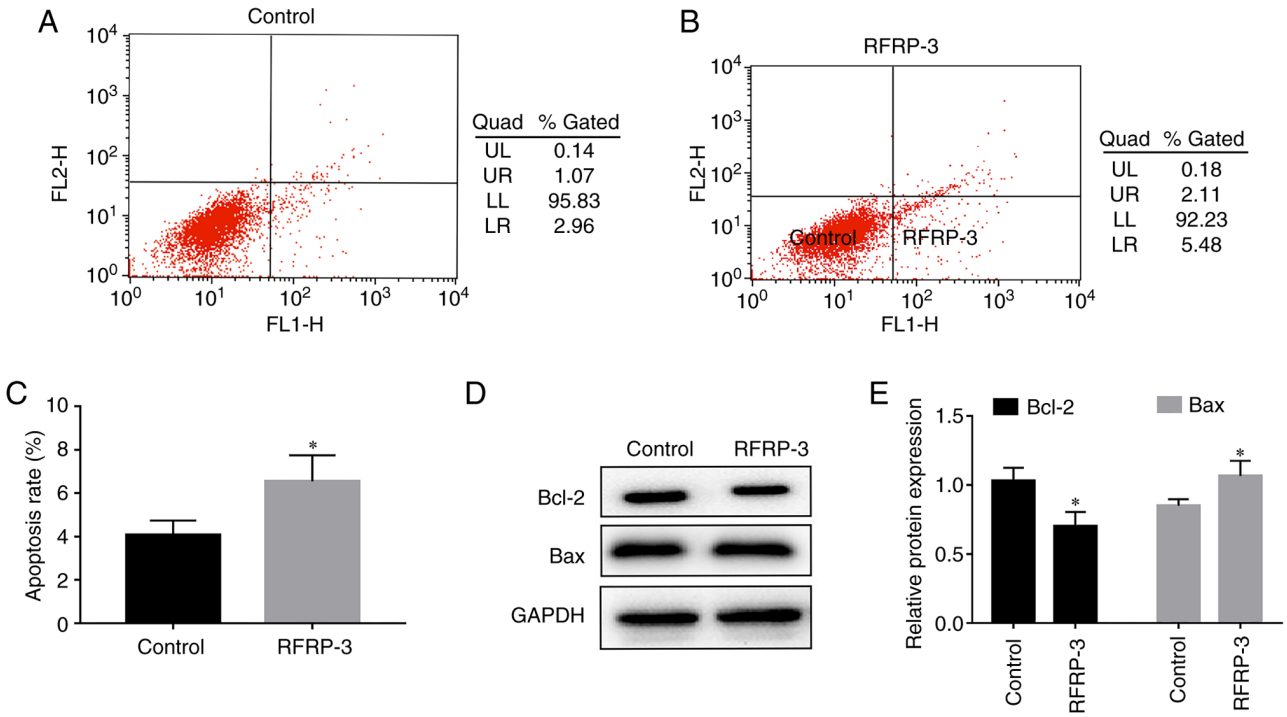


Figure 7. Effects of RFRP-3 on HEC-1A cell apoptosis. Percentage of apoptotic cells in the (A) control group and (B) the RFRP-3 group. (C) Comparison of apoptotic cell percentages between the RFRP-3 and control groups. (D) Western blot analysis of Bcl-2 and Bax protein expression. (E) Semi-quantification of Bcl-2 and Bax expression levels presented as relative expression. *P<0.05 vs. control. RFRP-3, RFamide-related peptide 3.

expressed in the hypothalamus, pituitary, ovaries, testis and uterus (30). Hinuma *et al* (32) found that the GPR147 mRNA expression can be detected in the ovaries and uterus of rats. In the human hypothalamus, pituitary gland and in hormone cells, GPR147 mRNA can also be detected by *in situ* hybridization (27,33). Another study reported that GPR147 is expressed in normal human ovaries and granulosa-luteinizing cells (27). The localization pattern of RFRP-3/GPR147 in mammals therefore provides a basis for its participation in regulating reproductive function. RFRP-3 mRNA can be detected in the uterus of juvenile sheep (29) and sows (31), where it may exert functional effects on the reproductive function and the development of uterus. GPR147 is extensively expressed throughout the mammalian uterus, suggesting that GnIH can regulate uterus function and ultimately reproductive function.

GnIH has been shown to mediate a number of functions on energy balance, nutrient availability and reproduction.

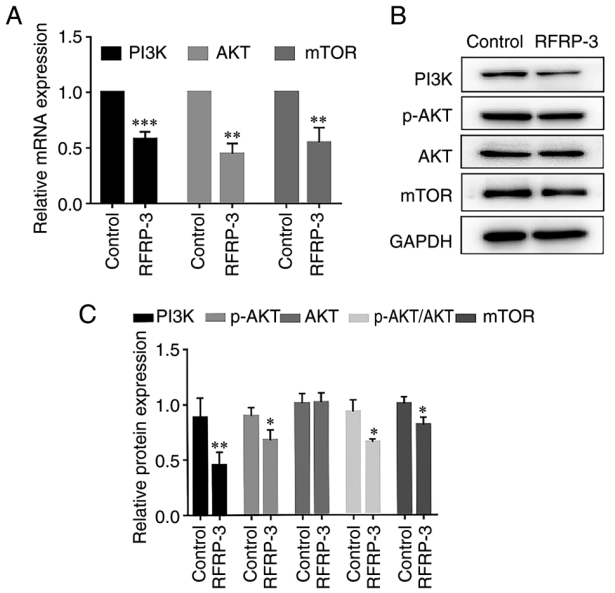


Figure 8. Effects of RFRP-3 on the PI3K/AKT/mTOR pathway in HEC-1A cells. HEC-1A cells in the RFRP-3 group were treated with 10,000 ng/ml RFRP-3 for 24 h. (A) The mRNA expression levels of PI3K, AKT and mTOR were measured by reverse transcription-quantitative PCR. (B) The protein expression levels of PI3K, AKT and mTOR, in addition to AKT phosphorylation, were measured using western blot analysis. (C) Semi-quantification of PI3K, AKT and mTOR expression, as well as AKT phosphorylation, presented as relative expression. $^{*}$P<0.05, $^{**}$P<0.01 and $^{***}$P<0.001 vs. control. RFRP-3, RFamide-related peptide 3; p, phosphorylated.

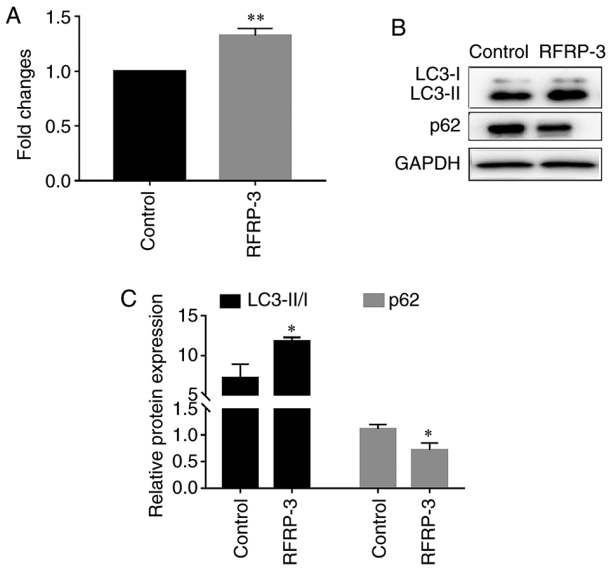


Figure 9. Effects of RFRP-3 on the expression of LC3-II and p62 in HEC-1A cells. HEC-1A cells were treated with 10,000 ng/ml RFRP-3 for 24 h. (A) The mRNA expression levels of LC3-II were detected by reverse transcription-quantitative PCR. (B) The protein expression levels of LC3-II and p62 were measured by western blot analysis. (C) Semi-quantification of LC3-II/I ratio and p62 expression level, presented as relative expression. $^{*}$P<0.05 and $^{**}$P<0.01 vs. control. RFRP-3, RFamide-related peptide 3.

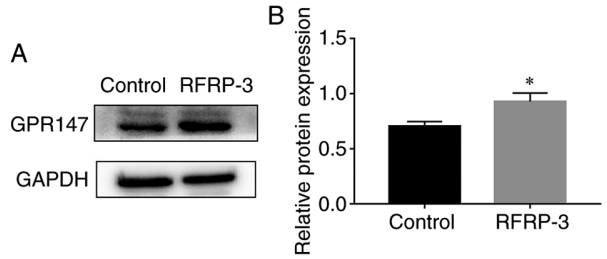


Figure 10. Effects of RFRP-3 on the protein expression level of GPR147 in HEC-1A cells. HEC-1A cells were treated with 10,000 ng/ml RFRP-3 for 24 h. (A) The protein expression level of GPR147 was measured using western blot analysis. Since the GPR147 antibody used was a polyclonal antibody, it may produce non-specific bands (top band). (B) Semi-quantification of GPR147 expression, presented as relative expression. $^{*}$P<0.05 vs. control group (mean ± SD of control, 0.7027±0.02529; mean ± SD of RFRP-3, 0.9254±0.04641). RFRP-3, RFamide-related peptide 3; GPR147, G protein-coupled receptor 147.

To ensure species continuity, successful reproduction relies on the tightly regulated balance of hormones in the HPG axis (1). Various factors, including the external environment, individual energy state and social relationships, can influence the HPG axis and reproductive function through various neuroendocrine systems. GnRH has been recognized to be a key stimulus for normal reproduction in animals. This is achieved by stimulating gonadotropin secretion, enhancing gonadal development, promoting the synthesis of sex steroid hormones and facilitating gamete production (4-6). By contrast, GnIH serves an important role in suppressing reproduction in the central nervous system. It can act directly on both hypothalamic GnRH and pituitary neurons through GPR147 to inhibit the production of gonadotropins, such as FSH and LH, and suppress reproduction (33,34). Johnson *et al* (36) previously revealed that administering GnIH in male rats through the ICV route can suppress sexual behaviors. In addition, Piekarski *et al* (37) reported that the ICV administration of GnIH can decrease the extent of vaginal scent marking and sexual motivation in female hamsters. Administering GnIH has also been shown to change Fos expression levels in the medial amygdala, medial preoptic area, critical neural loci and the stria terminalis bed nucleus, which are associated with female sexual behaviors (37). These aforementioned findings suggest that GnIH is heavily involved in modulating reproductive and feeding behaviors. Qi *et al* (38) found that GnIH neurons can project onto NPY, POMC and melanin-concentrating hormone neurons to regulate the feeding behavior (38). Consistent with this observation, administering GnIH through the ICV route can elevate food consumption in rats (36) and sheep (39). In addition, ICV injection of RFRPs has been found to promote the release of adrenocorticotropic hormone and oxytocin, which induces anxious behavior in rats (40). These findings suggest that GnIH can act on neurons in the brain to regulate various physiological functions. RFRP-3 is a HPG axis inhibitor that has been previously demonstrated to exert various regulatory functions on mammalian reproduction (1). However, information on RFRP-3 remains limited and the molecular mechanism of RFRP-3 in the female reproductive organs remain to be fully elucidated.

The uterus is an important reproductive organ in females. In particular, the uterine epithelium can be modulated by steroids to synthesize and/or secrete specific proteins into the uterine fluid, which serve important roles in reproductive processes, such as fertilization, embryo implantation and pregnancy maintenance (41,42). One method of studying the

reproductive process is by analyzing the protein components contained within the uterine fluid and their function. To explore the role of GnIH on protein synthesis in the uterus and in reproduction, the DEPs in the uterine fluid samples were screened using LC-MS/MS. Compared with the those in OEP rats without GnIH/RFRP-3 injection, GnIH/RFRP-3 injection through the lateral ventricle exerted an important effect on the protein composition and expression in the uterine fluid of OEP rats, suggesting that GnIH/RFRP-3 can act on the uterus by inhibiting the HPG axis. To explore the mechanism by which GnIH/RFRP-3 regulates uterus function on a molecular level, bioinformatics analysis was performed to analyze the role of DEPs. According to GO analysis, these DEPs were mostly enriched in 'extracellular region' and 'membrane-bounded vesicle' (CC), 'protein binding', 'protein complex binding' and 'macromolecular complex binding' (MF). In terms of BP, these DEPs mainly participated in 'response to organic substance', 'regulation of biological quality' and 'response to oxygen-containing compound'. These results suggest that GnIH/RFRP-3 treatment can affect protein binding. In addition, these DEPs were found to participate in protein, polypeptide and carbohydrate metabolism. Furthermore, these proteins showed association with antioxidation and were indicated to regulate cell proliferation, apoptosis, cell migration, cell adhesion and angiogenesis. According to PPI network analysis, the DEPs may participate in 'gap junction' and 'regulation of actin cytoskeleton'. In addition, these DEPs are likely to be involved in 'glycolysis/gluconeogenesis', 'carbon metabolism', 'biosynthesis of amino acids', 'long-term depression', 'thyroid hormone synthesis' and 'platelet activation'. Glycolysis, carbon metabolism and amino acid biosynthesis serve to provide energy for cells. After GnIH/RFRP-3 treatment, glycolysis becomes the main method of energy metabolism in cells, suggesting a close relationship with tumorigenesis (43,44). In addition, glycolysis has been shown to sperm maturation, motility and ultimately male reproduction by providing lactic acid or ATP (45,46). In addition, glycolysis can significantly affect the nuclear maturation in oocytes (47), suggesting that GnIH/RFRP-3 can regulate the development of uterus through the glycolytic pathway. Platelet activation is beneficial to tumor growth, angiogenesis and metastasis (48), suggesting that increased GnIH/RFRP-3 can affect the occurrence and development of tumors, which may have various clinical implications. GnIH/RFRP-3 treatment was found to affect the thyroid hormone synthesis pathway. Thyroid hormone can regulate metabolism and development in the ovary, uterus and placenta (49). It has been previously found that the GnIH mRNA expression is increased in the hypothalamus region of female hypothyroid mice (50), suggesting that GnIH/RFRP-3 treatment can regulate the development of uterus and female reproduction by affecting the synthesis of thyroid hormone.

In total, five hub proteins, namely Gna13, Gnaq, Gnai3, Kras and MMP9, were obtained based on PPI network analysis in the present study. The Ras family of genes, Hras, Kras and Nras represent the most commonly mutated oncogenes in human malignancies (51). Kras mutations have been associated with poor prognosis and treatment resistance in tumors (51). Accumulating evidence has shown that the Kras mutation is associated with cell proliferation and apoptosis, which upregulates estrogen receptor levels in endometrial cells (51-53). Furthermore, Kras appears to be directly associated with type I EC (51-53). In the present study, GnIH/RFRP-3 treatment reduced the expression levels of Kras. Therefore, it can be hypothesized that GnIH/RFRP-3 can downregulate the expression levels of Kras, thereby affecting the uterus and the occurrence/development of EC through the HPG axis. These five hub proteins were also associated with the platelet activation signaling pathway. It can be seen from the PPI network that the DEPs Gna 13, Gnaq and Gnai3 participate in the platelet activation pathway. When searching 'platelet activation' in the KEGG pathway database, the results showed that the DEPs were mostly associated with the 'platelet activation pathway', the activation of which affects the activity of adenylyl cyclase (AC)/cAMP/protein kinase A (PKA) signaling. Previous findings have shown that kisspeptin is co-expressed with GnIH/RFRP-3 within the neurons in the DMH area of Sprague-Dawley rats, where the direct interaction between recombinant RFRP-3 and kisspeptin was found using surface plasmon resonance (54). Therefore, GnIH/RFRP-3 may inhibit the expression of kisspeptin by inhibiting the AC/cAMP/PKA signaling pathway, further inhibiting the HPG reproductive axis to the uterus. GnIH has been shown to suppress AC/cAMP/PKA signal transduction (28,55,56). In addition, it has been found that there is an association between kisspeptin and ERK and cAMP/PKA pathway activation (57,58). The formation and development of EC is a complex process that involves interactions among multiple signal transduction pathways and genetic abnormalities (51-53). Therefore, it is necessary to perform further experiments to determine the effects of GnIH/RFRP-3 on EC. In the present study, to verify if the effects of RFRP-3 on the viability and apoptosis of HEC-1A cells were mediated by the hub proteins, further experiments were performed.

Using the UALCAN database to assess the expression profiles of the hub proteins, the expression of Gna13, Gnaq, Kras and MMP9 was found to be significantly changed in EC compared with that in normal samples. Gna13 is a member of the G protein G12 subfamily and is highly expressed in breast and prostate cancer (59). In addition, it has been previously associated with tumor metastasis and progression (60). Muralidharan *et al* (61) found the expression of Gna13 in EC tissues to be increased compared with that in normal tissues. However, the opposite result was obtained in UCLUAN database analysis. Thus, the role of Gna13 in EC remains controversial (60), which warrants further study. By contrast, Padol *et al* (62) found a significant decrease in Gnaq protein expression in the uterus of hypercholesterolemic mice (62), a condition that has been found to indirectly increase the risk of EC (63). Gnai3 is expressed to varying degrees in the mammalian uterus, the decreased expression of which has been indicated to result in the abnormal asymmetric division of stem cells *in vivo* (64). The disturbance of this balance not only affects normal development and growth but can also lead to cancer-associated cell hyperproliferation (64-67). MMP9 is associated with tumor growth, apoptosis, angiogenesis and metastasis; it has been reported to be overexpressed in EC, where it is also associated with disease progression (68-71).

The Kras gene is one of the most frequently mutated oncogenes in cancer, which is regularly associated with poor prognosis and treatment resistance (51). Previous studies (52,53) have suggested that Kras mutations are associated with cell proliferation and apoptosis, thereby upregulating the expression of estrogen receptors in endometrial cells. In addition, Kras appears to be directly associated with type I EC (52,53).

By contrast, Gnaq and MMP9 may be associated with proliferation in EC (62,68-71), which is inconsistent with the results of CCK-8 assay in the present study, where GnIH reduced HEC-1A cell viability. Indeed, RFRP-3 at 10,000 ng/ml inhibited the viability of HEC-1A cells. Compared with that in the control group, the apoptotic rate in RFRP-3 group was increased, whereas the expression of Bcl-2 was decreased and that of Bax was increased. Kras was selected for further study, since its protein expression levels were increased in the tumor compared with normal tissues in TCGA database analysis, whereas it was decreased in OEP rat uterine fluid after the ICV injection of RFRP-3.

Western blotting revealed that RFRP-3 at 10,000 ng/ml inhibited Kras expression. RFRP-3 reduced the expression of components in the PI3K/AKT/mTOR pathway in both mRNA and protein levels in HEC-1A cells. It has been shown that hyperactivation of the PI3K/AKT/mTOR pathway is associated with the pathogenesis of EC, whereas inhibition of the PI3K/AKT/mTOR pathway has important therapeutic significance (72). Therefore, RFRP-3 may inhibit the viability of HEC-1A EC cells whilst promoting apoptosis by inhibiting the PI3K/AKT/mTOR pathway. mTOR serves an important role in regulating autophagy in tumor cells (73). As in the present study RFRP-3 was found to decrease mTOR, the expression of autophagy markers LC3-II and p62 were detected (74). The results showed that 10,000 ng/ml RFRP-3 increased the ratio of LC3-II/ I whilst decreasing the expression of p62, suggesting enhanced autophagy activity (74). We hypothesize that the inhibitory effects of RFRP-3 on HEC-1A cells may be mediated by activating the GPR147 receptor, which promotes the hub protein Kras to activate the downstream PI3K/AKT/mTOR pathway, thereby reducing the expression of Bcl-2, whilst promoting the expression of Bax and inducing autophagy.

There are a number of limitations in the present study. For the validation of the proteomics analysis, several of the proteins identified via LC-MS/MS analysis should have been confirmed by western blot analysis. In addition, although GnIH/RFRP-3 may inhibit the immediate peripheral effects on vertebrate gonads, the specificity and sensitivity of GnIH/RFRP-3 in tissues and cells needs to be further verified. To enhance the consistency between *in vivo* and *in vitro* experiments, primary human endometrial epithelial cell lines should be used instead of EC cells. The cell cycle progression, immunohistochemistry, LC3 puncta and autophagic flux should also be measured.

In summary, the present study showed that RFRP-3 affects the uterus by upregulating MMP9 whilst downregulating Gna13, Gnaq, Gnai3 and Kras expression. In addition, RFRP-3 inhibited the viability but promoted the apoptosis of HEC-1A cells. These results can encourage the further exploration into the underlying molecular mechanism of the effects of GnIH/RFRP-3 on the uterus and provide novel ideas for the treatment of patients with EC.

**Acknowledgements**

Not applicable.

**Funding**

The present study was supported by the National Natural Science Foundation of China (grant nos. 81441133 and 81703001), Natural Science Foundation of Hebei Province (grant no. H2013406115), the Plan Project of Hebei Provincial Science and Technology Department (grant no. 08276101D-20), Hebei Higher Education Research Project (grant no. QN2015121) and Key Discipline of College and Universities in Hebei Province [grant. no. (2013)04; title, Pathogenic Biology].

**Availability of data and materials**

The datasets used and/or analyzed during the current study are available from the corresponding author on reasonable request. The proteomics datasets generated and/or analyzed during the current study are available in the iProX database (https://www.iprox.cn/; Project ID, IPX0005261000; https://www.iprox.cn//page/project.html?id=IPX0005261000).

**Authors' contributions**

LC and SY directed and designed the study. XZ wrote the manuscript. XZ, MW, LN, FW, LS and XL performed the experiments. XZ and LS confirm the authenticity of all the raw data. ZC and YQ analyzed the bioactive compounds using high-performance liquid chromatography. All authors have read and approved the final manuscript.

**Ethics approval and consent to participate**

All experiments involving animals were approved by The Experimental Animal Welfare Ethics Committee of Chengde Medical University (Chengde, China; approval no. CDMULAC-201808-003).

**Patient consent for publication**

Not applicable.

**Competing interests**

The authors declare that they have no competing interests.

**References**

1. Wang X, Guo GL, Zhang X, Li M, Xiao K, Hu C and Li X: Effect of RFRP-3, the mammalian ortholog of GnIH, on the epididymis of male rats. Theriogenology 118: 196-202, 2018.
2. Tsutsui K: A new key neurohormone controlling reproduction, gonadotropin inhibitory hormone (GnIH): Biosynthesis, mode of action and functional significance. Prog Neurobiol 88: 76-88, 2009.
3. Kriegsfeld LJ, Mei DF, Bentley GE, Ubuka T, Mason AO, Inoue K, Ukena K, Tsutsui K and Silver R: Identification and characterization of a gonadotropin-inhibitory system in the brains of mammals. Proc Natl Acad Sci USA 103: 2410-2415, 2006.

4. Tsutsui K, Bentley GE, Bedecarrats G, Osugi T, Ubuka T and Kriegsfeld LJ: Gonadotropin-inhibitory hormone (GnIH) and its control of central and peripheral reproductive function. Front Neuroendocrinol 31: 284-295, 2010.
5. Kriegsfeld LJ, Jennings KJ, Bentley GE and Tsutsui K: Gonadotrophin-inhibitory hormone and its mammalian ortholog RFamide-related peptide-3: Discovery and functional implications for reproduction and stress. Neuroendocrinol 30: e12597, 2018.
6. Tsutsui K, Ubuka T, Son YL, Bentley GE and Kriegsfeld LJ: Contribution of GnIH research to the progress of reproductive neuroendocrinology. Front Endocrinol (Lausanne) 6: 179, 2015.
7. Han X, He Y, Zeng G, Wang Y, Sun W, Liu J, Sun Y and Yu J: Intracerebroventricular injection of RFRP-3 delays puberty onset and stimulates growth hormone secretion in female rats. Reprod Biol Endocrinol 15: 35, 2017.
8. Chen L, Si LN, Wei M, Guo S, Yang SH, Chen ZH, Cheng LY and Qiao YB: Effects of GnIH on hypothalamic POMC positive neurons in ovariectomized rats supplemented with estrogen. Chin J Neuroanatomy 35: 57-63, 2019 (In Chinese).
9. Su W, Wei M, Feng C, Yang ZJ, Chen XY, Cheng LY, Yang SH and Qiao YB: Changes of neuropeptide Y mRNA and protein expression in hypothalamus of rats after intracerebroventricular injection of GnIH. Shandong Med J 56: 27-28, 2016 (In Chinese).
10. Wei M, Si LN, Chen L, Yang SH, Cheng LY and Qiao YB: Regulating effects of GnIH on POMC in hypothalamus of OEP rats. J Chengde Med College 34: 458-460, 2017 (In Chinese).
11. Chen WP, Witkin JW and Silverman AJ: Beta-Endorphin and gonadotropin-releasing hormone synaptic input to gonadotropin-releasing hormone neurosecretory cells in the male rat. J Comp Neurol 286: 85-95, 1989.
12. Fetissov SO, Kopp J and Hokfelt T: Distribution of NPY receptors in the hypothalamus. Neuropeptides 38: 175-188, 2004.
13. Morelli A, Marini M, Mancina R, Luconi M, Vignozzi L, Fibbi B, Filippi S, Pezzatini A, Forti G, Vannelli GB and Maggi M: Sex steroids and leptin regulate the 'first Kiss' (KiSS 1/G-protein-coupled receptor 54 system) in human gonadotrop in-releasing-hormone-secreting neuroblasts. J Sex Med 5: 1097-1113, 2008.
14. Braun MM, Overbeek-Wager EA and Grumbo RJ: Diagnosis and management of endometrial cancer. Am Fam Physician 93: 468-474, 2016.
15. Gompel A: Progesterone and endometrial cancer. Best Pract Res Clin Obstet Gynaecol 69: 95-107, 2020.
16. Corzo C, Barrientos Santillan N, Westin SN and Ramirez PT: Updates on conservative management of endometrial cancer. J Minim Invasive Gynecol 25: 308-313, 2018.
17. Emons G and Gründker C: The role of gonadotropin-releasing hormone (GnRH) in endometrial cancer. Cells 10: 292, 2021.
18. Grundker C, Gunthert AR, Westphalen S and Emons G: Biology of the gonadotropin-releasing hormone system in gynecological cancers. Eur J Endocrinol 146: 1-14, 2002.
19. Emons G, Grundker C, Gunthert AR, Westphalen S, Kavanagh J and Verschraegen C: GnRH antagonists in the treatment of gynecological and breast cancers. Endocr Relat Cancer 10: 291-299, 2003.
20. Fister S, Günthert AR, Aicher B, Paulini KW, Emons G and Gründker C: GnRH-II antagonists induce apoptosis in human endometrial, ovarian, and breast cancer cells via activation of stress-induced MAPKs p38 and JNK and proapoptotic protein Bax. Cancer Res 69: 6473-6481, 2009.
21. Livak KJ and Schmittgen TD: Analysis of relative gene expression data using real-time quantitative PCR and the 2(-Delta Delta C(T)) Method. Methods 25: 402-408, 2001.
22. Ukena K and Tsutsui K: A new member of the hypothalamic RF-amide peptide family, LPXRF-amide peptides: Structure, localization and function. Mass Spectrom Rev 24: 469-486, 2005.
23. Tsutsui K and Ukena K: Hypothalamic LPXRF-amide peptides in vertebrates: Identification, localization and hypophysiotropic activity. Peptides 27: 1121-1129, 2006.
24. Tsutsui K: How to contribute to the progress of neuroendocrinology: New insights from discovering novel neuropeptides and neurosteroids regulating pituitary and brain functions. Gen Comp Endocrinol 227: 3-15, 2016.
25. Tsutsui K and Ubuka T: GnIH control of feeding and reproductive behaviors. Front Endocrinol (Lausanne) 7: 170, 2016.
26. Ukena K, Iwakoshi E, Minakata H and Tsutsui K: A novel rat hypothalamic RFamide-related peptide identified by immunoaffinity chromatography and mass spectrometry. FFBS Lett 512: 255-258, 2002.
27. Ubuka T, Morgan K, Pawson AJ, Osugi T, Chowdhury VS, Minakata H, Tsutsui K, Millar RP and Bentley GE: Identification of human GnIH homologs, RFRP-1 and RFRP-3, and the cognate receptor, GPR147 in the human hypothalamic pituitary axis. PLoS One 4: e8400, 2009.
28. Ubuka T, Inoue K, Fukuda Y, Mizuno T, Ukena K, Kriegsfeld LJ and Tsutsui K: Identification, expression, and physiological functions of Siberian hamster gonadotropin-inhibitory hormone. Endocrinology 153: 373-385, 2012.
29. Li H: The expression of RFRP-3 in lamb tissue uses and its role between nutrition and reproduction (unpublished PhD thesis). Nanjing Agricultural University, 2014.
30. Liu J: The cloning mRNA expression of GnIH and its receptors in rabbit (unpublished PhD thesis). Nanjing Agricultural University, 2011.
31. Li X, Su J, Lei Z, Zhao Y, Jin M, Fang R, Zheng L and Jiao Y: Gonadotropin-inhibitory hormone (GnIH) and its receptor in the female pig: cDNA cloning, expression in tissues and expression pattern in the reproductive axis during the estrous cycle. Peptides 36: 176-185, 2012.
32. Hinuma S, Shintani Y, Fukusumi S, Iijima N, Matsumoto Y, Hosoya M, Fujii R, Watanabe T, Kikuchi K, Terao Y, *et al*: New neuropeptides containing carboxy-terminal RFamide and their receptor in mammals. Nat Cell Biol 2: 703-708, 2000.
33. Ubuka T, Son YL, Bentley GE, Millar RP and Tsutsui K: Gonadotropin-inhibitory hormone (GnIH), GnIH receptor and cell signaling. Gen Comp Endocrinol 190: 10-17, 2013.
34. Bonini JA, Jones KA, Adham N, Forray C, Artymyshyn R, Durkin MM, Smith KE, Tamm JA, Boteju LW, Lakhlani PP, *et al*: Identification and characterization of two G protein-coupled receptors for neuropeptide FF. J Biol Chem 275: 39324-39331, 2000.
35. Son YL, Ubuka T, Millar RP, Kanasaki H and Tsutsui K: Gonadotropin-inhibitory hormone inhibits GnRH-induced gonadotropin subunit gene transcriptions by inhibiting AC/cAMP/PKA-dependent ERK pathway in LβT2 cells. Endocrinology 153: 2332-2343, 2012.
36. Johnson MA, Tsutsui K and Fraley GS: Rat RFamide-related peptide-3 stimulates GH secretion, inhibits LH secretion, and has variable effects on sex behavior in the adult male rat. Horm Behav 51: 171-180, 2007.
37. Piekarski DJ, Zhao S, Jennings KJ, Iwasa T, Legan SJ, Mikkelsen JD, Tsutsui K and Kriegsfeld LJ: Gonadotropin-inhibitory hormone reduces sexual motivation but not lordosis behavior in female Syrian hamsters (Mesocricetus auratus). Horm Behav 64: 501-510, 2013.
38. Qi Y, Oldfield BJ and Clarke IJ: Projections of RFamide-related peptide-3 neurons in the ovine hypothalamus, with special reference to rigions regulating energy balance and reproduction. J Neuroendocrinol 21: 690-697, 2009.
39. Clarke IJ, Smith JT, Henry BA, Oldfield BJ, Stefanidis A, Millar RP, Sari IP, Chng K, Fabre-Nys C, Caraty A, *et al*: Gonadotropin-inhibitory hormone is a hypothalamic peptide that provides a molecular switch between reproduction and feeding. Neuroendocrinology 95: 305-316, 2012.
40. Kaewwongse M, Takayanagi Y and Onaka T: Effects of RFamide-related Peptide (RFRP)-1 and RFRP-3 on oxytocin release and anxiety-related behaviour in rats. J Neuroendocrinol 23: 20-27, 2011.
41. Lee RS, Wheeler TT and Peterson AJ: Large-format, two-dimensional polyacrylamide gel electrophoresis of ovine periimplantation uterine luminal fluid proteins: Identification of aldose reductase, cytoplasmic actin, and transferrin as conceptus-synthesized proteins. Biol Reprod 59: 743-752, 1998.
42. Cheng LY, Yang SH, Sun TC, Wang XQ, Hu W, Qi XW and Yu HM: Identification of an unknown uterine estrogen reactive protein ULF-250. Chin J Biochem Mol Biology 25: 60-64, 2009 (In Chinese).
43. Fuller GG and Kim JK: Compartmentalization and metabolic regulation of glycolysis. J Cell Sci 134: jcs258469, 2021.
44. Vettore L, Westbrook RL and Tennant DA: New aspects of amino acid metabolism in cancer. Br J Cancer 122: 150-156, 2020.
45. Narisawa S, Hecht NB, Goldberg E, Boatright KM, Reed JC and Millán JL: Testis-specific cytochrome c-null mice produce functional sperm but undergo early testicular atrophy. Mol Cell Biol 22: 5554-5562, 2002.
46. Boussouar F and Benahmed M: Lactate and energy metabolism in male germ cells. Trends Endocrinol Metab 15: 345-350, 2004.

47. Alvarez GM, Casiró S, Gutnisky C, Alvarez G, Dalvit GC, Sutton-McDowall ML, Thompson JG and Cetica PD: Implications of glycolytic and pentose phosphate pathways on the oxidative status and active mitochondria of the porcine oocyte during IVM. Theriogenology 86: 2096-2106, 2016.
48. Ren J, He J, Zhang H, Xia Y, Hu Z, Loughran P, Billiar T, Huang H and Tsung A: Platelet TLR4-ERK5 axis facilitates NET-Mediated capturing of circulating tumor cells and distant metastasis after surgical stress. Cancer Res 81: 2373-2385, 2021.
49. Silva JF, Ocarino NM and Serakides R: Thyroid hormones and female reproduction. Biol Reprod 99: 907-921, 2018.
50. Haraguchi S, Hara S, Ubuka T, Mita M and Tsutsui K: Possible role of pineal allopregnanolone in Purkinje cell survival. Proc Natl Acad Sci USA 109: 21110-21115, 2012.
51. Sideris M, Emin EI, Abdullah Z, Hanrahan J, Stefatou KM, Sevas V, Emin E, Hollingworth T, Odejinmi F, Papagrigoriadis S, *et al*: The Role of KRAS in endometrial cancer: A mini-review. Anticancer Res 39: 533-539, 2019.
52. Bulsa M and Urasińska E: Triple negative endometrial cancer. Ginekol Pol 88: 212-214, 2017.
53. Vitale SG, Valenti G, Gulino FA, Cignini P, Biondi A: Surgical treatment of high stage endometrial cancer: Current perspectives. Updates Surg 68: 149-154, 2016.
54. Cheng L, Yang S, Si L, Wei M, Guo S, Chen Z, Wang S and Qiao Y: Direct effect of RFRP-3 microinjection into the lateral ventricle on the hypothalamic kisspeptin neurons in ovariectomized estrogen-primed rats. Exp Ther Med 23: 24, 2022.
55. Son YL, Ubuka T and Tsutsu K: Molecular mechanisms of gonadotropin-inhibitory Hormone(GnIH) actions in target cells and regulation of GnIH expression. Front Endocrinol (Lausanne) 10: 110, 2019.
56. Son YL, Ubuka T, Soga T, Yamamoto K, Bentley GE and Tsutsui K: Inhibitory action of gonadotropin-inhibitory hormone on the signaling pathways induced by kisspeptin and vasoactive intestinal polypeptide in GnRH neuronal cell line,GT1-7. FASEB J 30: 2198-2210, 2016.
57. Sukhbaatar U, Kanasaki H, Mijiddorj T, Oride A and Miyazaki K: Kisspeptin induces expression of gonadotropin-releasing hormone receptor in GnRH-producing GT1-7 cells overexpressing G protein-coupled receptor 54. Gen Comp Endocrinol 194: 94-101, 2013.
58. Hara T, Kanasaki H, Tumurbaatar T, Oride A, Okada H and Kyo S: Role of Kisspeptin and Kiss1R in the regulation of prolactin gene expression in aat somatolactotroph GH3 cells. Endocrine 63: 101-111, 2019.
59. Rasheed SAK, Teo CR, Beillard EJ, Voorhoeve PM and Casey PJ: MicroRNA-182 and microRNA-200a control G-protein subunit α-13(GNA13) expression and cell invasion synergistically in prostate cancer cells. J Biol Chem 288: 7986-7995, 2013.
60. Muhammad S, Tang Q, Wei L, Zhang Q, Wang G, Muhammad BU, Kaur K, Kamchedalova T, Gang Z, Jiang Z, *et al*: miRNA-30d serves a critical function in colorectal cancer initiation, progression and invasion via directly targeting the GNA13 gene. Exp Ther Med 17: 260-272, 2019.
61. Jayaraman M, Radhakrishnan R, Mathews CA, Yan M, Husain S, Moxley KM, Song YS and Dhanasekaran DN: Identification of novel diagnostic and prognostic miRNA signatures in endometrial cancer. Genes Cancer 8: 566-576, 2017.
62. Padol AR, Sukumaran VS, Sadam A, Kesavan M, Arunvikram K, Verma AD, Srivastava V, Panigrahi M, Singh TU, Telang AG, *et al*: Hypercholesterolemia impairs oxytocin-induced uterine contractility in late pregnant mouse. Reproduction 53: 565-576, 2017.
63. Staff S, Aaltonen M, Huhtala H, Pylvänäinen K, Mecklin JP and Mäenpää J: Endometrial Cancer risk factors among lynch syndrome women: A retrospective cohort study. Br J Cancer 115: 375-381, 2016.
64. Martin-Belmonte F and Perez-Moreno M: Epithelial cell polarity, stem cells and cancer. Nat Rev Cancer 12: 23-38, 2012.
65. Knoblich JA: Asymmetric cell division: Recent developments and their implications for tumour biology. Nat Rev Mol Cell Biol 11: 849-860, 2010.
66. Gonzalez C: Spindle orientation, asymmetric division and tumour suppression in Drosophila stem cells. Nat Rev Genet 8: 462-472, 2007.
67. Williams ES, Ratliff AL, Postiglione MP, Knoblich JA and Fuchs E: Par3-mInsc and Gαi3 cooperate to promote oriented epidermal cell divisions through LGN. Nat Cell Biol 16: 758-769, 2014.
68. Karahan N, Güney M, Baspinar S, Oral B, Kapucuoglu N and Mungan T: Expression of gelatinase (MMP-2 and MMP-9) and cyclooxygenase-2(COX-2) in endometrial cancer. Eur J Gynaecol Oncol 28: 184-188, 2007.
69. Iurlaro M, Loverro G, Vacca A, Cormio G, Ribatti D, Minischetti M, Ria R, Bruno M and Selvaggi L: Angiogenesis extent and expression of matrix metalloproteinase-2 and -9 correlate with upgrading and myometrial invasion in endometrial cancer. Eur J Clin Invest 29: 793-801, 1999.
70. Graesslin O, Cortez A, Fauvet R, Lorenzato M, Birembaut P and Daraï E: Metalloproteinase-2, -7 and -9 and tissue inhibitor of metalloproteinase-1 and -2 expression in normal, hyperplastic and neoplastic endometrium: A clinical-pathological correlation study. Ann Oncol 17: 637-645, 2006.
71. Srdelić Mihalj S, Kuzmić-Prusac I, Zekić-Tomaš S, Šamija-Projić I and Čapkun V: Lipocalin-2 and matrix metalloproteinase-9 expression in high-grade endometrial cancer and their prognostic value. Histopathology 67: 206-215, 2015.
72. Barra F, Evangelisti G, Ferro Desideri L, Di Domenico S, Ferraioli D, Vellone VG, De Cian F and Ferrero S: Investigational PI3K/AKT/mTOR inhibitors in development for endometrial cancer. Expert Opin Investig Drugs 28: 131-142, 2019.
73. Wullschleger S, Loewith R and Hall MN: TOR signaling in growth and metabolism. Cell 124: 471-484, 2006.
74. Vishnupriya S, Priya Dharshini LC, Sakthivel KM and Rasmi RR: Autophagy markers as mediators of lung injury-implication for therapeutic intervention. Life Sci 260: 118308, 2020.